



Title	Low-temperature-sensitivity heterostructure photonic-crystal wavelength-selective filter based on ultralow-refractive-index metamaterials
Author(s)	Florous, NI; Saitoh, K.; Koshiba, M.
Citation	Applied Physics Letters, 88(12), 121107-1-121107-3 https://doi.org/10.1063/1.2188055
Issue Date	2006-03-20
Doc URL	http://hdl.handle.net/2115/8400
Rights	Copyright © 2006 American Institute of Physics
Type	article
File Information	ApplPhysLett_88_121107.pdf



[Instructions for use](#)

Low-temperature-sensitivity heterostructure photonic-crystal wavelength-selective filter based on ultralow-refractive-index metamaterials

Nikolaos Ioannou Florous,^{a)} Kunimasa Saitoh, and Masanori Koshiba

Division of Media and Network Technologies, Hokkaido University, Sapporo 060-0814, Japan

Maksim Skorobogatiy

Genie Physique, Ecole Polytechnique de Montreal, Centre-ville Montréal C.P. 6079, Canada

(Received 6 July 2005; accepted 22 February 2006; published online 21 March 2006)

We propose and numerically investigate the thermal-insensitive properties of a wavelength-selective filter based on heterostructure photonic crystals with ultralow-refractive-index metallic nanowires. The operational principle of the proposed device is based on the photon trapping by total external reflections between the ultralow refractive index metamaterial claddings and the guiding air cores. The low propagation losses, the ultracompact size as well as the temperature-insensitive operation are the main advantages of the proposed metamaterial technology, making the proposed de-multiplexer an excellent candidate for applications in nanophotonic-integrated systems operating in the visible frequency spectrum. © 2006 American Institute of Physics.

[DOI: 10.1063/1.2188055]

Recently, photonic crystals (PCs), which are morphologically periodic electromagnetic media, witnessed an unpredicted development in which a variety of unusual electromagnetic phenomena have been discovered. Most of the unusual properties of PCs are based on the modification or, in some cases, the extinction of the density of the electromagnetic states, inside the crystal.¹

A key component in the design of reconfigurable optical communication systems is a wavelength selective filter (WSF), since it can divide and combine different wavelength channels, each carrying an optical signal. The concept of realizing ultracompact WSF circuits based on the extraordinary properties of PCs for telecommunication applications has recently been proposed.^{2,3} However, employing PC devices based on usual semiconducting materials is challenging for dense integration at visible frequencies (400–700 nm), due to the fact that dielectric materials are suffering from inhomogeneous imperfections in their own atomic structure resulting in high losses and fabrication difficulties. In addition, their material properties are sensitive to environmental temperature changes,⁴ frequently necessitating employment of a temperature maintaining environment.

The inclusion of metals in PCs, operating at visible frequencies, has been suggested to offer some advantages over semiconductors, due to their surprising metamaterial properties. Moreover, in the visible frequency regime, despite their lossy nature, metals can increase the size of the photonic band gaps without introducing significant losses.^{5–9} One of the appealing properties of metal-based PCs is the increased temperature stability as will be demonstrated in this letter. The mechanism of confining light in these structures consists of trapping the photons in the air core between low-refractive index composite metallic claddings, by total external reflections.⁵ In addition, these metallic composites can be engineered to show an equivalent homogenous refractive

index lower than the air or even with negative values (metamaterials).

We believe that metal based metamaterials can have a significant impact in the design of nanophotonic integrated circuits in the visible frequency band. In this letter we perform numerical characterization using a rigorous scattering matrix technique,^{10–14} of a three-color planar heterostructure PC-WSF circuit, operating on the principle of total external reflection mechanism, having low losses as well as temperature-insensitive propagation characteristics. The wavelength selectivity of the proposed device is achieved by varying the size of the metallic nanopillars in consecutive homogenous sections in a PC heterostructure. With the presence of the metallic heterostructure, we can control the equivalent low refractive index of the composite cladding, by a judicious choice of the radius and the lattice constant of the individual PC units. The optimized performance of the device in terms of transmission characteristics is ensured with the modification of the add-drop PC channel dimensions. Thus the cross talk between the add-drop channels is minimized by using a topological optimization strategy.¹⁵

Consider the PC structure as shown in Fig. 1. It is composed of metallic nanowires (rods) in a triangular array with lattice constant Λ . The metallic rods in the consecutive heterostructure PCs have different radii in an ascending order of

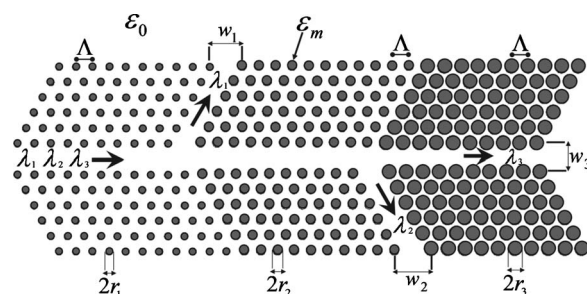


FIG. 1. Topology of a three-channel H-PC de-multiplexer composed of metallic nanowires embedded in air.

^{a)} Author to whom correspondence should be addressed; electronic mail: nflorous@dpo7.ice.eng.hokudai.ac.jp

r_j , $j=1,2,3$. The background material is air, while the nano-rods can be of any metallic material. Until recently, only a simplified temperature-independent Drude model for the characterization of metals at optical frequencies has been used,^{6–8,16} thus prohibiting the study of temperature-depending phenomena in metallic PCs. To model more accurately the behavior of metals at visible frequencies, and to take into account the impact of possible temperature variations, we have adopted an improved Drude model of metals¹⁷

$$\varepsilon_m = 1 - \varepsilon_\infty \frac{\omega_p^2 + v_c^2}{\omega^2 + v_c^2} + j\varepsilon_\infty \frac{\omega_p^2 + v_c^2}{\omega} \frac{v_c}{\omega^2 + v_c^2},$$

$$v_c(\omega, T) = v_{c0} \left[1 + \left(\frac{h\omega}{2\pi k_B T} \right)^2 \right], \quad (1)$$

where ε_∞ is the relative dielectric constant at high frequencies, ω_p is the plasma frequency, v_{c0} is the classical relaxation rate in the free electron model of metals, ω is the angular frequency, T is the absolute temperature, k_B is the Boltzmann constant, and h is the Planck's constant. Additionally, in our theoretical model we assume that the geometrical characteristics of the pillars will remain invariant as the temperature changes and only the permittivity function is affected. This approximation can be verified to hold for most metals around room temperatures. To minimize as much as possible the material absorption by the metallic nanopillars, we have chosen copper (Cu) as a model metal, since copper introduces the smallest average material losses for the composite metamaterial claddings in the visible spectral band (400–700 nm), among other metals used in this frequency regime such as gold (Au) or silver (Ag).^{5,17,18} For copper the following parameters are considered: $\varepsilon_\infty \cong 0.9$, $\omega_p/2\pi = 1914$ THz and $v_{c0}/2\pi = 8.34$ THz.^{17,18}

Typically, in the case of a straight metallic PC waveguide, the total external reflection mechanism will guide only the fundamental TM-polarized mode.⁸ Cutoff frequencies of the guided modes can be modified by altering the size of the metallic rods, in the consecutive homogenous sections of the metallic PC. The ratio r_j/Λ , $j=1,2,3$, determines the magnitude of the equivalent refractive index of a composite metamaterial cladding, the lower the ratio the higher the effective refractive index.⁵ Thus, in a given homogenous lattice by altering the diameters of the nano-rods the cutoff frequency of the guided mode can be controlled.¹⁹ By increasing the size of the metallic nano-rods, the cutoff wavelength is shifted to lower wavelengths in the spectral band as a consequence of decreasing the equivalent refractive index of the metamaterial cladding. Therefore, as the diameter of metallic cylinders is increased in consecutive sections of the PC, the edge of the transmission band is shifted to shorter wavelengths. The dimensions of the add-drop waveguide channels have been modified using a topological optimization technique¹⁵ extended to the metallic PCs, to minimize the cross talk between the guiding channels. For demultiplexing visible frequencies, ranging from $\lambda=400$ nm (violet light) up to $\lambda=680$ nm (red light), the sizes of the rods and the pitch constants in the consecutive heterostructure sections were calculated using the described methodology and the requirement that the add-drop channels should drop out appropriate cutoff wavelengths. Optimized geometrical parameters were chosen as, $\Lambda=200$ nm, $r_1=40$ nm, $r_2=56$ nm, and $r_3=80$ nm. Based on these values, the real parts of the equivalent refractive indexes in the j th PC-block

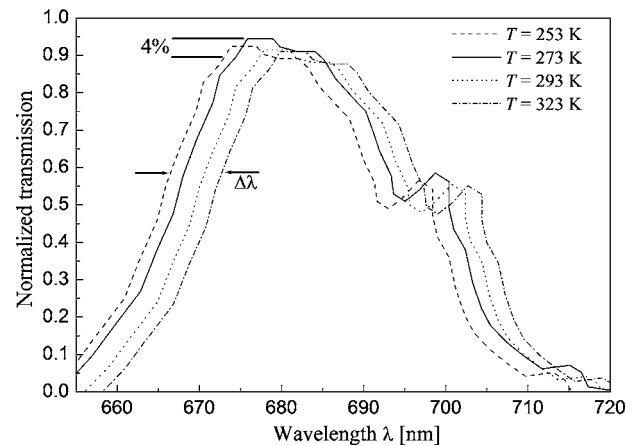
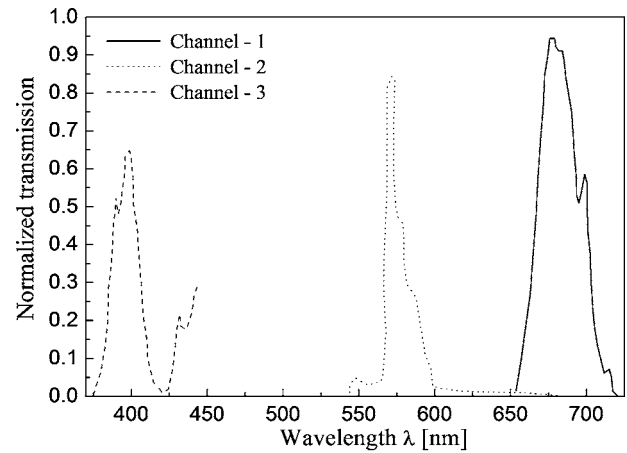


FIG. 2. Normalized transmission characteristics for (a) a system at $T=273$ K, (b) channel 1 at various temperatures. The total wavelength shift of the transmission for a temperature variance of $\Delta T = \pm 35$ K is $\Delta\lambda = \pm 3$ nm, with transmission loss variance of 4%, indicating a low-temperature sensitivity.

$j=1,2,3$, are approximately equal to 0.214 at $j=1$, 0.132 at $j=2$ and 0.1 at $j=3$ for fixed operating wavelength of $\lambda=678$ nm, while the optimized add-drop channel widths were determined by using a topological optimization technique¹⁵ to be, $w_1=371$ nm, $w_2=415$ nm, and $w_3=323.5$ nm.

In Fig. 2(a) we verify the de-multiplexing operation by plotting the TM-(incident electric field parallel to the metallic rods) transmission for the optimized structure at temperature $T=273$ K. Observe that the transmission losses increase for lower wavelengths as a consequence of increasing absorption in a metamaterial cladding, due to the increment of the imaginary part of the equivalent refractive index in the j th PC block. In Fig. 2(b) we demonstrate the impact of the temperature variation on the transmission characteristics of our device for the channel 1 in the temperatures range: $T=253$ – 323 K. From the results in Fig. 2(b) we conclude that a temperature change of $\Delta T = \pm 35$ K will result in a wavelength shift of $\Delta\lambda = \pm 3$ nm, in the transmission curve, which in normalized units is 0.085 nm/K near the room temperature range, while at the same time the transmission loss variance is about 4%. At this point it is necessary to compare our findings with the standard experimental measured sensitivities of usual tunable photonic crystals fabricated by using III-V material platforms. A temperature shift of $\Delta T = \pm 25$ K will typically produce a wavelength shift of $\Delta\lambda = \pm 4.75$ nm, which in normalized units is about 0.19 nm/K, for fabricated dielectric PCs operating in the telecommunication band.²⁰

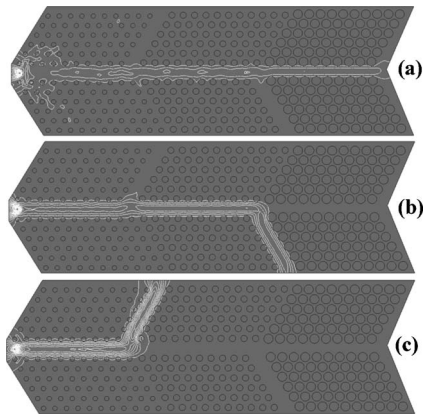


FIG. 3. Contour plot of the electromagnetic power flow in the heterostructure metallic PC de-multiplexer at (a) $\lambda_1=400$ nm (violet light), (b) $\lambda_2=570$ nm (yellow light), and (c) $\lambda_3=678$ nm (red light). The power penetration in the metamaterial claddings in the worst case of (a) (violet light) is less than -30 dB.

Theoretical estimates based on the shift of the photonic band gaps in usual dielectric PCs have shown a sensitivity of about 0.14 nm/K.²¹ Comparing these results with ours, we can see that our proposed metal-based device is significantly less sensitive to temperature fluctuations. Finally, in Fig. 3 we visualize the de-multiplexing operation by plotting the contour levels of the two-dimensional electromagnetic power flow at different wavelengths, at a fixed temperature of $T=273$ K; specifically, Fig. 3(a) shows the power localization at $\lambda_1=400$ nm (violet light), Fig. 3(b) shows the power localization at $\lambda_2=570$ nm (yellow light), and Fig. 3(c) shows the power localization at $\lambda_3=678$ nm (red light). To quantify the power leakage flow in the metamaterial claddings (only six rows of metallic cylinders were used to model the ultralow-refractive-index metamaterial claddings), we have estimated that in the worst case, which occurs at $\lambda_1=400$ nm (violet light) transmission, the portion of the electromagnetic power penetrating the low refractive index metamaterials is only -30 dB, a value that indicates a strong localization level of light, which can be considered acceptable for most practical applications.

In summary, we have theoretically introduced and numerically demonstrated the low-temperature-sensitivity operation of a novel type of heterostructure PC-WSF circuit, designed with ultralow-refractive-index metamaterial claddings, for applications in the visible spectrum. Low propaga-

tion losses, circuitry-size reduction,⁸ as well as temperature-insensitive operation are ensured by the inclusion of metallic nanowires into the compact-sized PC architecture. We believe that the proposed PC structure can be realized on the basis of recently reported experimental results of fabricated PC waveguide slabs composed of metallic nanowires.²² The proposed metamaterial technology can be employed in nanophotonic integrated systems operating, for example, as beam combiners or splitters in the visible spectrum, in three-dimensional holographic data storage devices using multiple laser sources, or as a delivery system for exciting quantum electrodynamics' cavities for nano-spectroscopy experiments.

¹E. Yablonovich, Phys. Rev. Lett. **58**, 2059 (1987).

²M. Koshiba, J. Lightwave Technol. **19**, 1970 (2001).

³B. S. Song, S. Noda, and T. Asano, Science **300**, 1537 (2003).

⁴C. S. Kee and H. Lim, Phys. Rev. B **64**, 121103 (2001).

⁵B. T. Schwartz and R. Piestun, J. Opt. Soc. Am. B **20**, 2448 (2003).

⁶V. Poborchii, T. Taya, T. Kanayama, and A. Moroz, Appl. Phys. Lett. **82**, 508 (2003).

⁷S. I. Bozhevolnyi, V. S. Volkov, K. Leosson, and A. Boltasseva, Appl. Phys. Lett. **79**, 1076 (2001).

⁸O. Takayama and M. Cada, Appl. Phys. Lett. **85**, 1311 (2004).

⁹A. Moroz, Phys. Rev. B **66**, 115109 (2002).

¹⁰D. Felbacq, G. Tayeb, and D. Maystre, J. Opt. Soc. Am. A **11**, 2526 (1994).

¹¹R. C. McPhedran, L. C. Botten, A. A. Asatryan, N. A. Nicorovici, P. A. Robinson, and C. M. Stekre, Phys. Rev. E **60**, 7614 (1999).

¹²D. Pissort, B. Denecker, P. Bienstman, F. Olyslager, and D. De Zutter, J. Opt. Soc. Am. A **21**, 2186 (2004).

¹³N. J. Florous and M. Koshiba, *The Third International Conference on Computational Electromagnetics and Its Applications*, Beijing, China, November 2004, No. ICCEA-2004, No. A1-004.

¹⁴N. J. Florous and M. Koshiba, Int. Photonics Res. Applications (IPRA-2005), ITuB3 (2005).

¹⁵P. I. Borel, A. Harpoth, L. H. Frandsen, M. Kristensen, P. Shi, J. S. Jensen, and O. Sigmund, Opt. Express **12**, 1996 (2004).

¹⁶V. Kuzmiak, A. A. Maradudin, and F. Pincemin, Phys. Rev. B **50**, 16835 (1994).

¹⁷*Optical Properties of Solids*, edited by F. Abeles (North-Holland, Amsterdam, 1972).

¹⁸*Handbook of Optical Constants of Solids*, edited by E. D. Palk (Academic, Orlando, 1988).

¹⁹M. Notomi, A. Shinya, K. Yamada, J. Takahashi, C. Takahashi, and I. Yokohama, IEEE J. Quantum Electron. **38**, 736 (2002).

²⁰Ch. Schuller, F. Klopff, J. P. Reithmaier, M. Kamp, and A. Forchel, Appl. Phys. Lett. **82**, 2767 (2003).

²¹P. Halevi and E. R. Mendieta, Phys. Rev. Lett. **85**, 1875 (2000).

²²A. Christ, S. G. Tikhodeev, N. A. Gippius, J. Kuhl, and H. Giessen, Phys. Rev. Lett. **91**, 183901 (2003).